

Supporting Information

**Silver Nanoparticles - Laser Induced Graphene (Ag NPs - LIG)
Hybrid Electrodes for Sensitive Electrochemical-Surface Enhanced
Raman Spectroscopy (SERS) Detection**

Yunyun Mu,^{a,b,†} Jahidul Islam,^{a,†} Richard Murray,^a Cathal Larrigy,^a Alida Russo,^a
Xinping Zhang,^b Aidan J. Quinn,^a Daniela Iacopino^{a*}

^aTyndall National Institute, University College Cork, Dyke Parade, Cork, Ireland

^bFaculty of Science, Institute of Information Photonics Technology, Beijing University
of Technology, Beijing 100124, China

† These two authors contributed equally

Details of custom-made EC-SERS cell

A custom-built electrochemical cell (76 width and 1.41 mm depth) was designed in FreeCad (v 0.19), sliced in Ultimaker Cura (v. 4.13.1) and fabricated using a filament 3D printer (Creality Ender 3, 0.4mm nozzle, 0.2mm layer height, 20% infill, 210 °C print temperature, 60mm/s print speed) using polylactic acid (Radionics, product number: 174-0002). The cell was composed of a series of wells to recess the sample, allowing deposition of 50 -70 μ L electrolyte volumes, and to allow the insertion of a coverslip to prevent contamination of the Raman objective. Through holes were included to allow the mounting of mechanical contact electrodes for interface with LIG electrodes. Electrodes were mounted in the recessed well. Two side extensions were built around the holder, on the left and right outer sides of the chamber, to allow space to ensure reproducible electrical connectivity between external press metal fingers and the LIG CE, WE and RE.

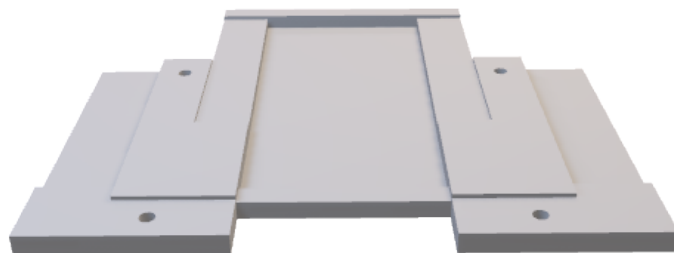


Figure S1. Custom Cell for EC-SERS analysis.

Characterization of Ag NPs

The as-prepared Ag NPs were characterized by an absorption band centered at 407 nm (see Figure S2a). Upon concentration (40 times), the solution displayed a deep grey color, as shown in the inset of Figure S2a. SEM images of the as prepared solution showed a distribution of shapes from spherical- to rod-like with an average size of 50 nm (Figure S2b).

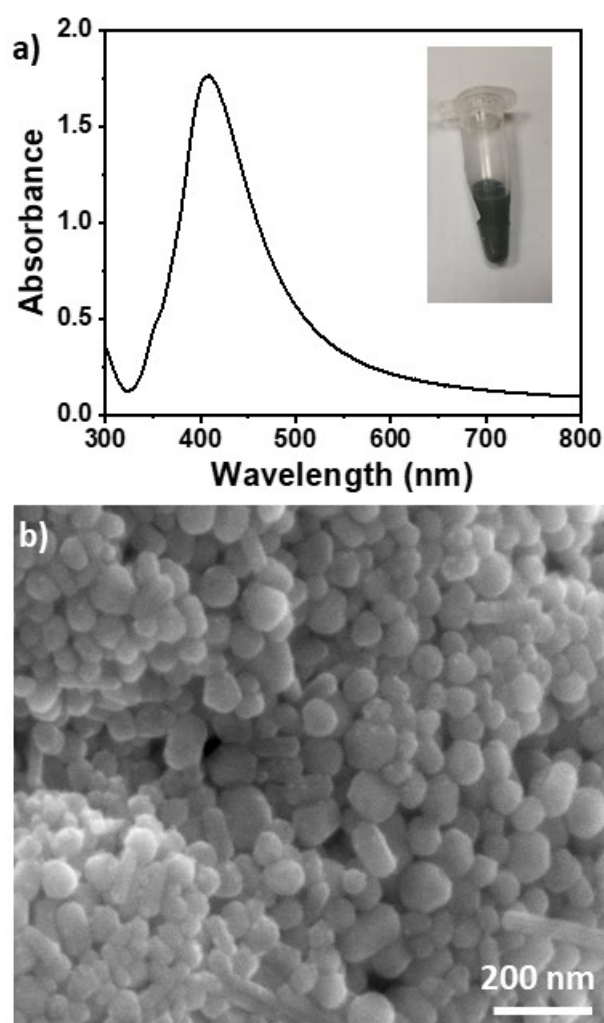


Figure S2. a) UV-vis spectrum of Ag NPs. Inset: photograph of Ag NPs concentrated 100 times; b) SEM image of Ag NPs.

SEM imaging of Ag NPs – LIG electrodes

Figure S3 shows low magnification SEM images of LIG structures obtained by direct laser writing of polyimide using lasers of different wavelengths. LIG structures obtained with a 405 nm laser (Figure S3a) showed well-defined LIG tracks corresponding to the laser raster scanning of the polyimide surface and constituted by quasi-hemispherical islands corresponding to individual pixels in the original design. Each pixel island had a diameter of ca. 100 μm . Figure S3b show SEM image of LIG structures obtained by polyimide writing with a 450 laser. In contrast with the smooth surface previously obtained at 405 nm, the trenches obtained at 450 nm displayed well defined tracks with open pores. A similar morphology was observed in the LIG structures obtained by 10.6 μm laser writing. The low magnification (Figure S3c) SEM image showed formation of narrow trenches corresponding to the raster scanning action of the laser.

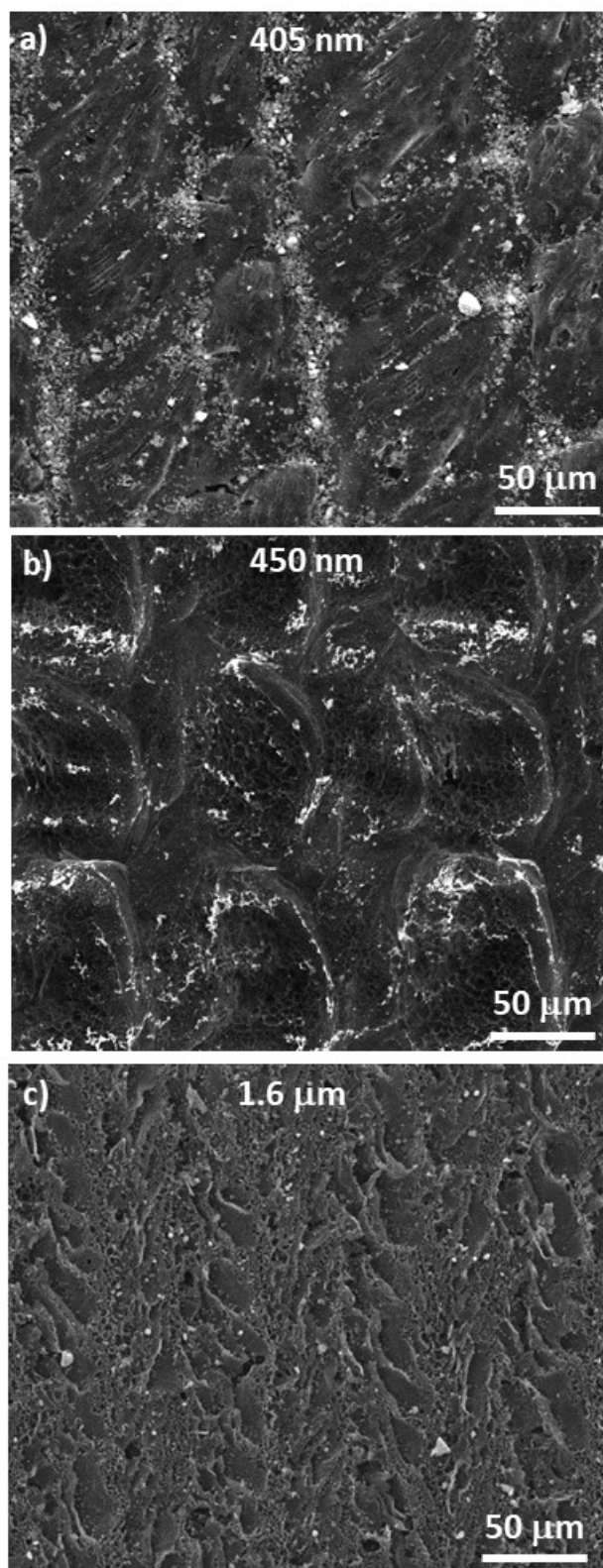


Figure S3. Low magnification SEM images of Ag NPs - LIG structures obtained by laser writing of polyimide sheets with different lasers: a) 405 nm; b) 450 nm; c) 10.6 μm .

4-ABT Raman/SERS peak assignment

Table. S1. Raman Band Frequencies of p-Aminothiophenol. Approximate description of the modes (ν , stretch; δ , γ and β bend).

Peak Position	Peak position	Assignments[1]	Peak position	Assignments[2]
4-ABT powder	4-ABT/Ag		DMAB/Ag	
1590		ν_{CC} , 8a (a1)		
	1578	ν_{CC} , 8b (b2)	1579	ν_{CC} (ag)
1492		$\nu_{CC} + \delta_{CH}$, 19a (a1)	1473	$\nu_{NN} + \beta_{CH}$ (ag)
	1436	$\nu_{CC} + \delta_{CH}$, 19b (b2)	1433	$\nu_{NN} + \beta_{CH}$ (ag)
	1388	$\delta_{CH} + \nu_{CC}$, 3 (b2)	1389	$\nu_{NN} + \nu_{CN}$ (ag)
			1303	
1287		ν_{CH} , 7a' (a1)		
1174	1188	δ_{CH} , 9a (a1)	1191	$\nu_{CN} + \beta_{CH}$ (ag)
	1142	δ_{CH} , 9b (b2)	1142	$\nu_{CN} + \beta_{CH}$ (ag)??
1084	1075	ν_{CS} , 7a (a1)	1075	$\nu_{CC} + \nu_{CS}$ (ag)
1005		$\gamma_{CC} + \gamma_{CCC}$, 18a (a1)		

[1] J. AM. CHEM. SOC. 2010, 132, 9244-9246

[2] Phys. Chem. Chem. Phys., 2012, 14, 8485-8497

4-ABT SERS

Figure S4 shows SERS spectra of 4-ABT (1×10^{-6} M) obtained with the different fabricated Ag NPs – LIG structures. Spectra were taken at random locations of the substrate. Their variability in intensity and response reflects well the variability of the substrate. For comparison, Figure S4d also shows comparative spectra of 4-ABT taken on Ag NPs deposited on glass substrate.

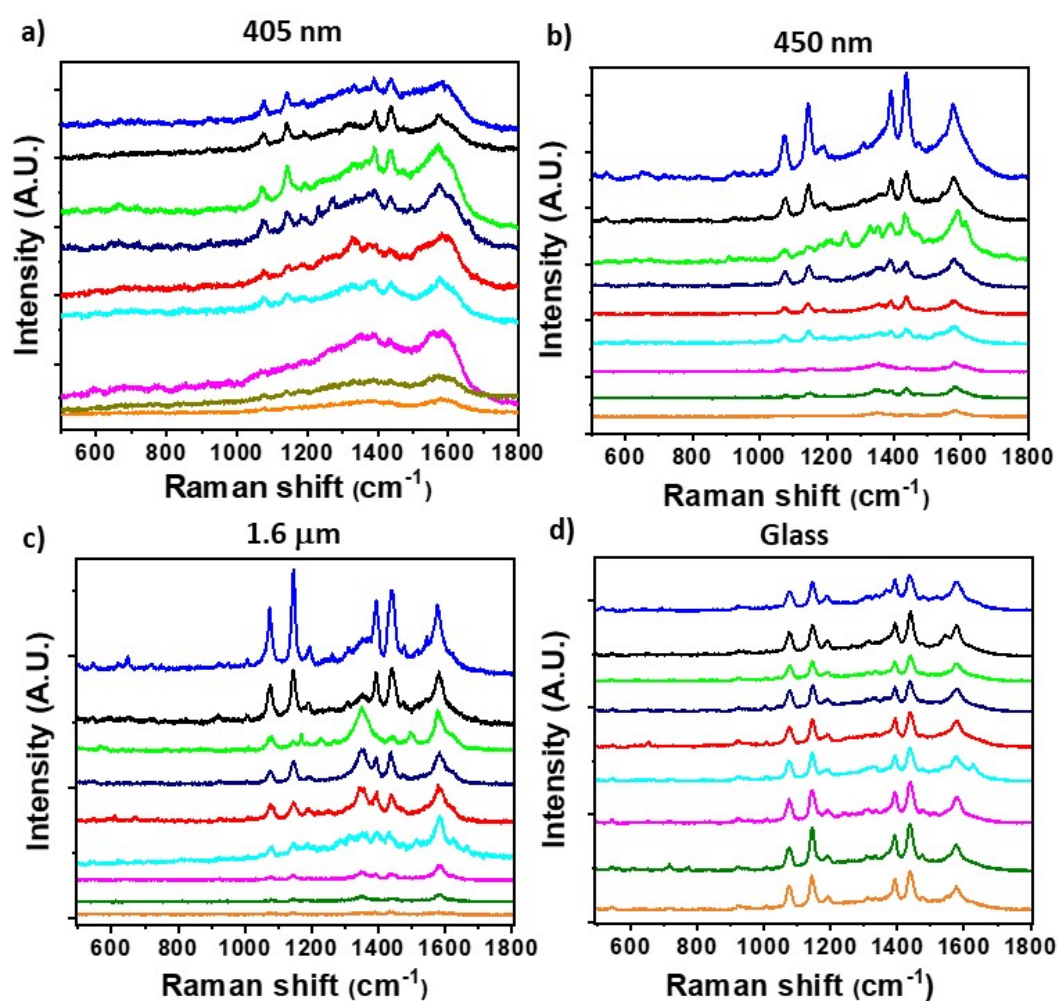


Figure S4. SERS spectra of 4-ABT taken at nine random locations on different substrates: a) Ag NPs – LIG 405 nm; b) Ag NPs – LIG 450 nm; c) Ag NPs – LIG 10.6 μm ; d) Ag NPs - glass.

Melamine Raman and SERS

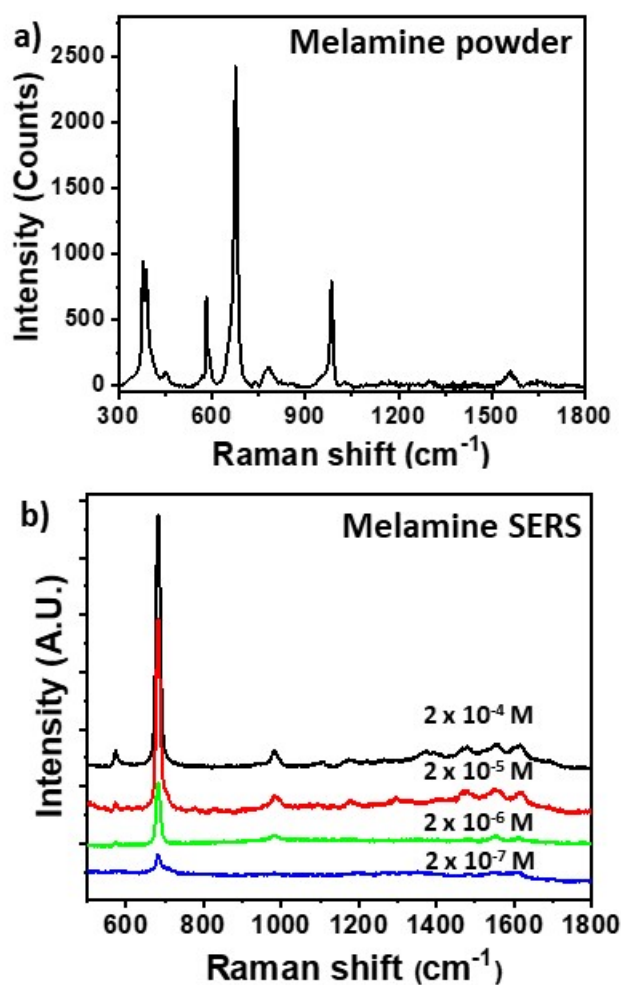


Figure S5. a) Raman spectrum of melamine powder; b) SERS spectrum of melamine solutions of different concentrations (PBS) deposited on Ag NPs – LIG 450 nm substrate. All spectra were recorded with 750 nm laser and 10 s integration time.

DIF Raman and SERS

The Raman spectrum of DIF powder is shown in Figure S6a (750 nm laser illumination). It showed peaks at 1307 cm^{-1} (pyrazine ring vibrations), 1393 cm^{-1} (ν_{ring} quinolone ring), 1463 and 1448 cm^{-1} assigned to the normal modes involving contributions from piperazine moiety and angular deformation from CH_2 and CH_3 groups, 1498 cm^{-1} (δ_{CH_2}), 1541 cm^{-1} (CO stretching mode of the carboxylate moiety $\nu_{\text{C=O}}$), 1629 cm^{-1} ($\nu_{\text{C=C}}$ aromatic ring).

Figure S6b shows the SERS spectra of DIF solution (1×10^{-3} M, $\text{H}_2\text{O}:\text{CH}_3\text{CN}$ 1:1) deposited on Ag NPs - LIG-450 nm measured by using 785 nm laser irradiation. Compared to the Raman spectrum, the intense SERS bands at 1546, 1340, 920, 785 and 548 cm^{-1} (related to C ring and carboxylate stretching) have significant contribution allowing to infer such molecular moieties are involved in the interaction with the metallic surface. Also, SERS peaks at 1625, 1340, 1051, 747 and 550 cm^{-1} (CC, CN stretching vibrations from aromatic rings) have important contributions suggesting an almost perpendicular orientation of these rings on the surface.

Figure S6c shows the SERS spectra of DIF solutions of various concentrations (400 ppm equal to 1×10^{-3} M) deposited on Ag NPs – LIG 450 nm substrate. Characteristic peaks of DIF were visible down to 0.4 ppm (0.4 mg/L).

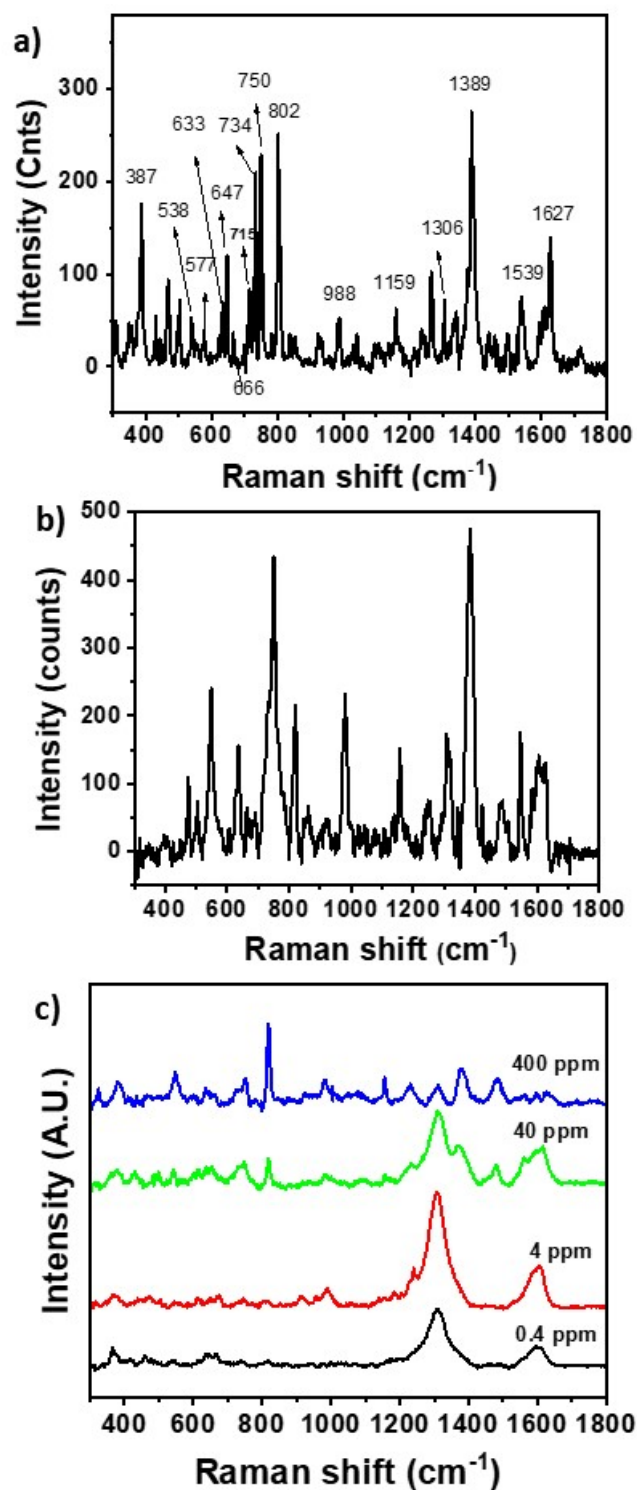


Figure S6. a) Raman spectrum of DIF powder; b) SERS spectrum of DIF deposited on Ag NPs – LIG 450 nm substrate; c) SERS spectra of DIF of different concentrations ($1 \times 10^{-3} - 1 \times 10^{-6}$ M) recorded on Ag NPs – LIG 450 nm substrate. All spectra were taken with 750 nm laser illumination.

Table. S2. Raman Band Frequencies of DIF. Approximate description of the modes (ν , stretch; δ , bend).

Peak Position	Peak position	Assignments
DIF powder	DIF/Ag	
1627	1625	$C=C_{\text{stretch}}$ (aromatic ring)
1539	1546	δCH_2
1389	1384	ν_{ring} (quinolone ring)
1306	1314	Mixed vibration (Pyrazine ring)